UDC 621.313.333-192

Goroshko Andrii.
Prof, Dr. Sc., Khmelnitsky National University, Ukraine
Reviewer: Vitaly Pavlovich Tkachuk, Ph.D. tech. Sciences, Associate Professor, Ukraine

Zembytska Maryna.
Assoc. Prof., Ph.D., Khmelnitsky National University, Ukraine

Simulation of induction motor vibrations under the Influence mechanical and magnetic eccentricity

Abstract. A mathematical model of the dynamics of an electric induction motor is proposed, taking into account the eccentricity of the mass of the rotor; static and dynamic magnetic eccentricities of the rotor, influence of the gyroscopic moment of the rotor; compliance of the stator supports to the foundation. The model has six stator degrees of freedom (three translational and three rotational) and two rotor stages. The model takes into account the uneven rigidity of the stator supports, their number and the places of attachment to the stator.

Keywords: Induction Motor, rigid rotor, Eccentricity of rotor mass, Magnetic eccentricity Unbalanced Magnetic Pull

Introduction

For induction motors, bearings fixed in special risers are used as rotor supports. The risers are bolted to the lower half of the end shield. For induction motors, bearing failures account for about 40% of the total number of failures [1]. The main factors of their increased wear are the mechanical imbalance of the rotor due to the eccentricity of the rotor mass and the unbalanced magnetic pull (UMP) due to the magnetic eccentricity. Because induction motors have a relatively small air gap, they are more prone to UMP. Dynamic forces and moments caused by the eccentricity of the rotor are additional internal excitation for the motor subsystem, which include centrifugal force (CF), friction-impact forces (RIF), UMP, unbalanced force torque and friction moment [2].

Mechanical imbalance occurs due to inevitable manufacturing deviations, inaccuracy of assembly and design features of the rotors, as a result of which the axial symmetry is broken and the center of inertia in some cross sections does not coincide with the geometric center of the sections and the axis of rotation of the rotor. Magnetic eccentricity and UMP causes an additional radial load on the bearing, which shortens its service life. In addition, UMP reduces the overall stiffness of the system, which can increase vibrations within the system [3].

According to various sources, eccentricity accounts for 20 to 40% of motor failures [4-6]. The reasons for the appearance of magnetic eccentricity and unevenness of the air gap are due to errors during the production and assembly of the machine, as well as unfavorable conditions of its operation [7].

Distinguish between static and dynamic eccentricity. Static eccentricity occurs due to the eccentric position of the rotor in the stator bore, so the non-uniform air gap configuration does not change with time as the rotor rotates. The static eccentricity of the air gap must exceed 10% [2]. With dynamic eccentricity due to the eccentric position of the rotor relative to the stator axis, the configuration of the air gap changes during the rotation of the rotor, which is due to the rotation of the rotor axis relative to the stator axis. Given the small size of the air gap of the motor, even a slight eccentricity of the rotor, violating the symmetry of the machine design, significantly impairs its operation. Therefore, the timely detection of eccentricity at the early stages of its development is of great practical importance and is one of the important tasks of monitoring the technical condition of the motor and diagnosing defects.

Many authors [1-8] conduct research on the creation of mathematical models that most effectively describe the rotor dynamics of motor. In the well-known models developed in the above works, it is assumed that the inertia is concentrated in a plane that divides the length of the rotor in half, and the eccentricity of the mass causes a centrifugal force, under the action of which the rotor performs only translational movements. In this article, the task was to develop a model with an arbitrary location of the center of mass of the rotor. This makes it possible to take into account static, torque and dynamic imbalance, taking into account the torque forces of the imbalance, and, accordingly, the rotational movements of the stator.

Mathematical model of motor oscillations with mass eccentricity

In the proposed model, the absolutely rigid body of the motor stator has six degrees of freedom and can perform translational motion in the directions of the axes x, y, z, as well as rotations around these axes. The rotor, rotating with an angular velocityω, can make small translational movements in the direction of the x and z axes. The stator-rotor system has a total of 8 degrees of freedom.

In the model shown in fig. 2, the following assumptions are made:

- elastic characteristics of all supports are linear;
- rotor is considered rigid and its deformations are neglected;
- position of the center of mass of the rotor is known.

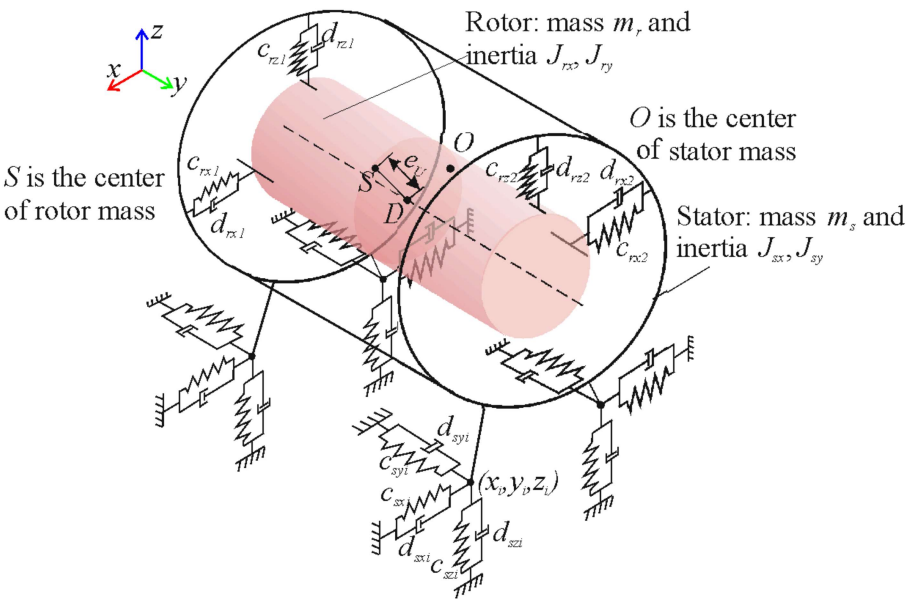

Fig. 1. Dynamic model of an induction motor with rotor mass eccentricity

To specify the position in space of this system, it is necessary to have eight generalized coordinates. For such coordinates we take three Cartesian coordinates of the center of inertia of the stator of the machine x, y, z, three angles α, β, γ, which specify the rotations of these coordinate axes rigidly connected to the stator and two coordinates of the center of inertia of the rotor x_r, z_r,. In these coordinates, the stator oscillations can be represented as a superposition of six helical movements with fixed axes of the screws x, y, z. The stator generally performs six-chain oscillations. The static eccentricity is $e_U = SD$. Dynamic eccentricity DO is determined by the coordinates point $D(x_D,y_D,z_D)$, obtained by the intersection of the axis of rotation of the rotor with a plane drawn through the center of the mass S perpendicular to the axis of rotation of the rotor.

The differential equations of oscillations of the motor system are based on the Lagrange equation of the second kind and take into account the energy dissipation during Rayleigh damping:

$$\frac{d}{dt}\left(\frac{\partial T}{\partial \dot{q}_j}\right) - \frac{\partial T}{\partial q_j} + \frac{\partial V}{\partial q_j} + \frac{\partial D}{\partial \dot{q}_j} = 0,\ j = 1,2,...,8, \tag{1}$$

where j=1,2,…,8 is the number of generalized coordinates.

Performing mathematical operations for the Lagrange equation (1) in eight generalized coordinates x, y, z, α, β, γ, x_r, z_r and setting $\omega = const$ we obtain a system of eight differential equations in matrix form:

$$\mathbf{M}\ddot{\mathbf{q}} + (\mathbf{G} + \mathbf{D})\dot{\mathbf{q}} + \mathbf{A}\mathbf{q} = \mathbf{Q}, \quad (2)$$

where $\mathbf{M} = \left[m_{ij} \right]_1^8$ is the matrix of inertial coefficients;

$\mathbf{G} = \left[g_{ij} \right]_1^6$ is the matrix of gyroscopic coefficients;

$\mathbf{D} = \left[\alpha_{ij} \right]_1^8$ is the matrix of damping coefficients;

$\mathbf{A} = \left[\alpha_{ij} \right]_1^8$ is the matrix of stiffness coefficients;

$\mathbf{q} = \left[x, y, z, \alpha, \beta, \gamma, x_r, z_r \right]^T$ is the column vector of generalized coordinates;

$\mathbf{Q} = \left[F_x, 0, F_z, M_x, M_y, M_z, F_x, F_z \right]^T$ is the column vector of generalized force factors.

The inertia matrix M contains the mass value of the rotor m_r and the mass value of the stator m_s their moments of inertia J_{sx}, J_{sy}, J_{rx}, J_{ry}. The damping matrix **A** contains the stiffness value of n stator-foundation supports $C_{sx_i}, C_{sy_i}, C_{sz_i}$, i=1…n, and m rotor-foundation supports $C_{rx_i}, C_{ry_i}, C_{rz_i}$, i=1…m. The damping matrix **D** contains the values of the damping coefficients of n stator-foundation supports $d_{sx_i}, d_{sy_i}, d_{sz_i}$, i=1…n, and m rotor-foundation supports $d_{rx_i}, d_{ry_i}, d_{rz_i}$, i=1…m and the coordinates of the connection of all supports.

Accounting for magnetic eccentricity in the model

Mixed magnetic eccentricity e_m is a combination of magnetic static and dynamic eccentricities. In the general case, it is not equal to the eccentricity of the mass e_U, since it characterizes the deviation of the magnetic centers of the stator and rotor, which may not coincide with the geometric center of the stator and the axis of rotation of the rotor, respectively. Static magnetic eccentricity e_{ms} creates a load on the rotor, which can be characterized by the resulting radial force acting on the minimum air gap. Dynamic eccentricity e_{md} creates a force vector that acts on the rotor and rotates at the speed of the rotor. The model in Fig. 1 dynamic magnetic eccentricity is taken into account by point D coordinates: $e_{md} = \sqrt{x_D^2 + z_D^2}$.

Since UMP does not depend on the parameters included in the model in Fig. 1, the effect of UMP can be taken into account by an additional radial nonlinear force F_{UMP} in the system of equations (2).

To estimate the UMP, we use the theoretical expressions proposed in [2, 9].

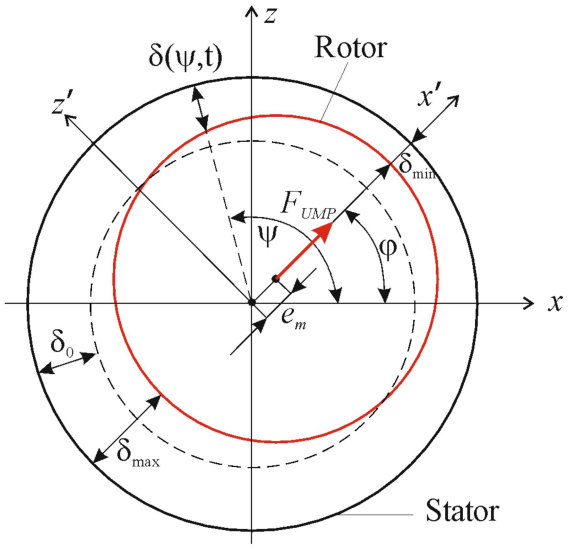

Fig. 2. Scheme of magnetic eccentricity of the rotor

The length of the air gap of the eccentric rotor according to the diagram in fig. 2 for any eccentricity at any time is approximately equal to:

$$\delta(\psi,t) \approx \delta_0 - e_m \cos(\psi - \varphi) \tag{3}$$

where δ_0 denotes the average air gap when centering the rotor (the mean air-gap length), ψ is the stator position angle, e_m is the magnetic eccentric distance of the rotor, ϕ is denotes the eccentric angle of the rotor.

With dynamic eccentricity and constant rotation speed ω=const, the position angle of the eccentricity is a function of time $\varphi = \varphi_0 + \omega t$, therefore

$$\delta(\psi,t) \approx \delta_0 - e_{md} \cos(\psi - \varphi_0 - \omega t), \tag{4}$$

where ϕ_0 is the initial angle of the dynamic eccentricity position, ω is angular speed of the rotor.

UMP is strongly nonlinear. Nonlinear UMP calculation methods use the energy method or the integration of the Maxwell stress tensor in the air gap between the stator and the rotor [8]. The UMP on the surface of the rotor can be calculated, respectively, as follows

$$F_{UMPx}=\begin{cases} f_1\cos\varphi+f_2\cos\left(2\omega_e t-\varphi\right)+f_3\cos\left(2\omega_e t-3\varphi\right), p=1,\\ f_1\cos\varphi+f_3\cos\left(2\omega_e t-3\varphi\right)+f_4\cos\left(2\omega_e t-5\varphi\right), p=2,\\ f_1\cos\varphi+f_4\cos\left(2\omega_e t-5\varphi\right), p=3,\\ f_1\cos\varphi,\ p\geq 4, \end{cases}$$

$$F_{UMPz}=\begin{cases} f_1\sin\varphi+f_2\sin\left(2\omega_e t-\varphi\right)+f_3\sin\left(2\omega_e t-3\varphi\right), p=1,\\ f_1\sin\varphi+f_3\sin\left(2\omega_e t-3\varphi\right)+f_4\sin\left(2\omega_e t-5\varphi\right), p=2,\\ f_1\sin\varphi+f_4\sin\left(2\omega_e t-5\varphi\right), p=3,\\ f_1\sin\varphi,\ p\geq 4, \end{cases} \tag{5}$$

where $F_{\mathrm{UMP}x}$ and $F_{\mathrm{UMP}z}$ are the force projections of UMP on the axis x and z respectively, ω_e is the angular frequency of the power source of the stator power, p denotes the number of pole pairs of the motor, f_1, f_2, f_3, f_4 – represent the magnetic pull amplitude, which are found by the formulas:

$$\begin{aligned} f_1&=\frac{Rl\pi}{4\mu_0}F_j^2\left(2\Lambda_0\Lambda_1+\Lambda_1\Lambda_2+\Lambda_2\Lambda_3\right),\\ f_2&=\frac{Rl\pi}{4\mu_0}F_j^2\left(\Lambda_0\Lambda_1+\frac{1}{2}\Lambda_1\Lambda_2+\frac{1}{2}\Lambda_2\Lambda_3\right),\\ f_3&=\frac{Rl\pi}{4\mu_0}F_j^2\left(\Lambda_0\Lambda_3+\frac{1}{2}\Lambda_1\Lambda_2\right),\\ f_4&=\frac{Rl\pi}{8\mu_0}F_j^2\Lambda_2\Lambda_3, \end{aligned} \tag{6}$$

where R and l are the radius and length of the rotor, F_j is the amplitude of the fundamental harmonic of the magneto motive force of the rotor excitation (MMF), μ_0 is the air permeance. The Fourier coefficients, Λ_i can be calculated as follows

$$\Lambda_i=\begin{cases} \dfrac{\mu_0}{\delta_0}\dfrac{1}{\sqrt{1-\varepsilon^2}},\ i=0,\\ \dfrac{2\mu_0}{\delta_0}\dfrac{1}{\sqrt{1-\varepsilon^2}}\left(\dfrac{1}{1+\sqrt{1-\varepsilon^2}}\right)^i,\ i>0. \end{cases} \tag{7}$$

where $\varepsilon=\dfrac{e_m}{\delta_0}$ indicates relative eccentricity.

The angular speed of rotation of the rotor, taking into account the slip s of the induction motor, is related to the angular speed of rotation of the magnetic field ω_{m} and the angular frequency of the electric current supplying the windings ω_{e}

$$\omega = (1-s)\omega_m = (1-s)\frac{\omega_e}{p} . \tag{8}$$

To take into account both the mechanical and magnetic eccentricity of the rotor a vector $\mathbf{Q}_{UMP} = \left[F_{UMPx}, 0, F_{UMPz}, 0, 0, 0, F_{UMPx}, F_{UMPz}\right]^T$ should be added to the vector of generalized force factors **Q** of system (2) and equation (2) will turn into

$$\mathbf{M}\ddot{\mathbf{q}} + (\mathbf{G} + \mathbf{D})\dot{\mathbf{q}} + \mathbf{A}\mathbf{q} = \mathbf{Q} + \mathbf{Q}_{UMP} , \tag{9}$$

Numerical Example Two-pole squirrel-cage induction motor was chosen for simulation. The power of the motor is 1,5 kW. The data of the induction motor and the bearings are listed in Table 1

.

Table 1. Parameters of the three-phase induction motor

Notation	Description	Value
	Motor data	
n	Rated speed (rpm)	3000
s	Rated slip	0,05
R	Radius of the rotor (мм)	0,11
l	Length of the rotor (m)	0,2
m_r	Mass of the rotor (kg)	3,6
m_s	Mass of the stator (kg)	14,2
δ_0	Mean air-gap length (мм)	0,4
μ_0	Air permeance (N/A^2)	$4\pi \cdot 10^{-7}$
F_j	Fundamental MMF amplitude of the rotor excitation current (A)	96,04
p	Number of pole pairs	1
C_{rx}, C_{rz}	Stiffness of bearing housing and end shield (N/m)	$4{,}6 \cdot 10^{-7}$
	Foundation data	
C_{sz}	Vertical stiffness of the foundation at each motor support (N/m)	$3{,}8 \cdot 10^{-6}$

C_{sx}	Horizontal stiffness of the foundation at each motor support (N/m)	$2{,}5 \cdot 10^{-6}$

In real induction motors, the center of mass may not lie in the *Oxz* plane. In order to take into account the spatial position of the eccentricity of the masses, the created model takes into account the additional degree of freedom of the stator along the *y* axis using the coordinate y_D. Further, the influence of the mismatch of the stator center of mass along the length of the rotor *l*, was studied, the results of which are presented in Fig. 1. The maximum value of longitudinal vibrations is observed at the critical frequency (Fig. 3). This is explained by an increase in the moment of action of the centrifugal force, which leads to an increase in angular oscillations relative to the *x* and *z* axes due to the action of generalized force factors along the coordinates α and γ: $M_x = m_r\omega^2 e_U y_D \cos\omega t$ and $M_x = -m_r\omega^2 e_U y_D \sin\omega t$. In this regards, the matrix of inertial coefficients **M** is not diagonal. An increase in angular vibrations causes an increase in the displacement of the stator due to the translational and rotational movement. These vibrations can negatively affect the performance of the bearing node and reduce its service life.

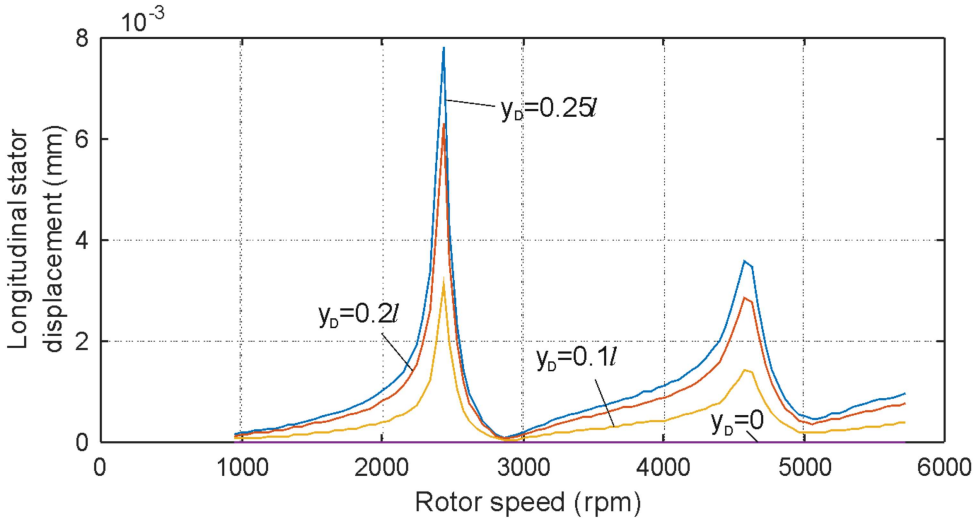

Fig. 3. Frequency response at variable displacement y_D (longitudinal vibration along the y axis)

In fig. 4 presents comparative dependences of horizontal transverse vibrations of the rotor at different types of eccentricity. The eccentricity location angle is equal to ϕ=45°. The value of the relative eccentricity is equal to ε=0.1.

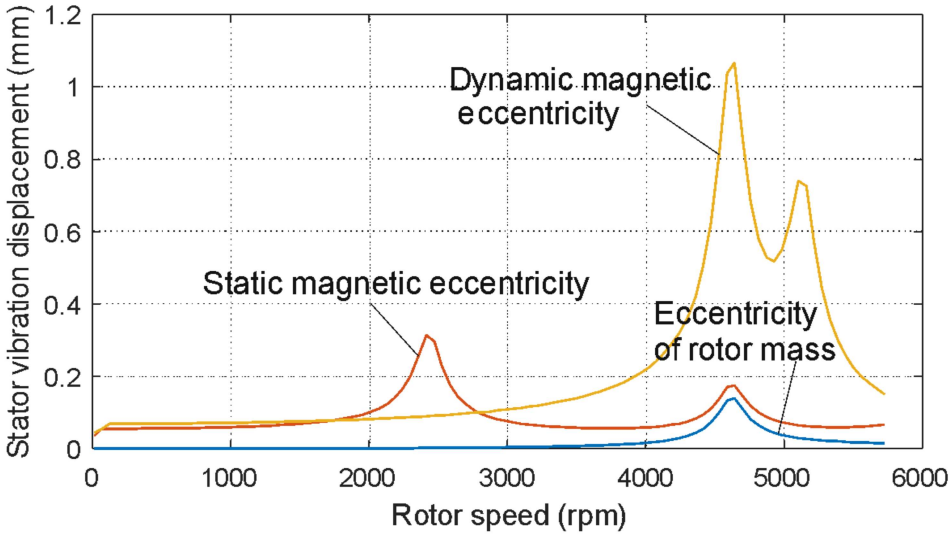

Fig. 4. Comparative frequency response of horizontal stator vibrations with different types of eccentricity of the rotor

In fig. 5 shows the distribution of the $F_{UMP,}$ which acts on the rotor at a speed of 2412 rpm due to static eccentricity during half the period of the electromagnetic field ω_e, which corresponds to the time $t = \frac{\pi}{\omega_e} = 12.4$ ms. Time dependences of the components F_{UMPx} and F_{UMPz} are presented in Fig. 6. F_{UMP} changes at twice the frequency of the current. Since p=1, this frequency is approximately 2 times higher than the speed of rotation of the rotor. The UMP spectrum contains zero frequency and frequency components $2\omega_e$.

In fig. 7 shows the distribution of the $F_{UMP,}$ acting on the rotor as a result of dynamic eccentricity during the time t=0.5 s. Time dependences of the components F_{UMPx} and F_{UMPz} are presented in Fig. 8. As a result of the precession of the rotor, F_{UMP} changes both with the frequency of the electromagnetic field ω_e and with the frequency of precession ω_e-ω.

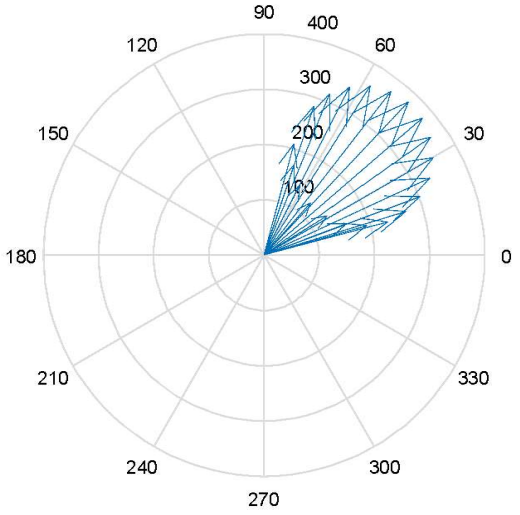

Fig. 5. F_{UMP} diagram. Static eccentricity ε=0.1, eccentric angle ϕ=45°

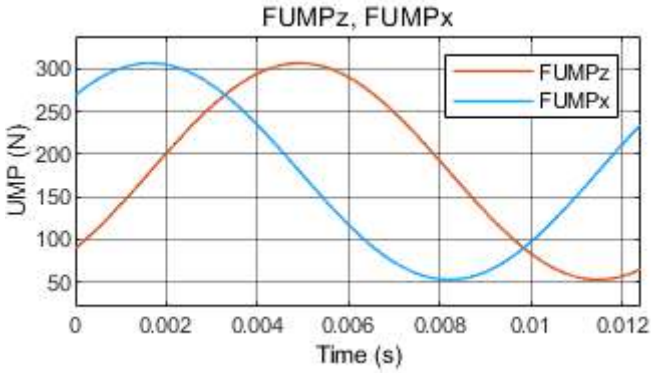

Fig. 6. Dependences of F_{UMP} components. Static eccentricity ε=0.1, eccentric angle ϕ=45°

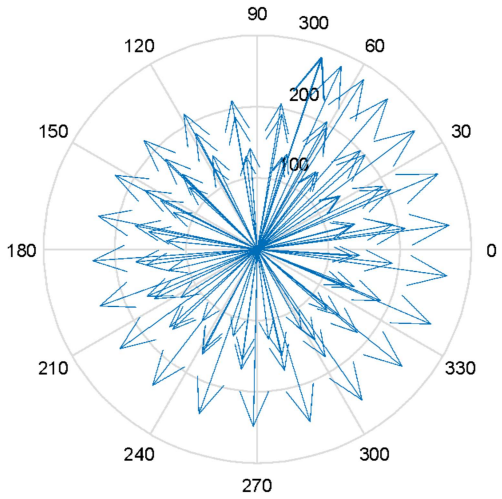

Fig. 7. F_{UMP} diagram. Dynamic eccentricity ε=0.1, eccentric angle ϕ_0=45°

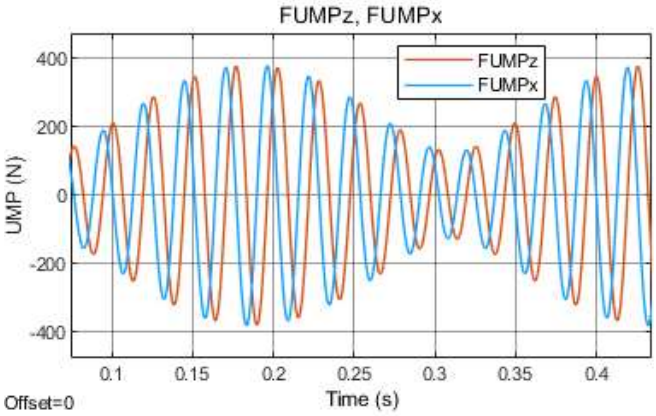

Fig. 8. Dependences of F_{UMP} components. Dynamic eccentricity ε=0.1, eccentric angle ϕ_0=45°

The unbalanced rotor force F caused by the mass eccentricity and the UMP force F_{UMP} caused by the dynamic eccentricity rotate at the speed of the rotor. The relative position of the eccentricities will affect the magnitude of the total unbalanced force, as shown in Fig. 9. The total force and amplitude of the vibrations can be maximized in the most unfavorable case, when both eccentricities are summed. The total force reaches a minimum if the eccentricities are subtracted, and this fact should be taken into account when balancing the rotor.

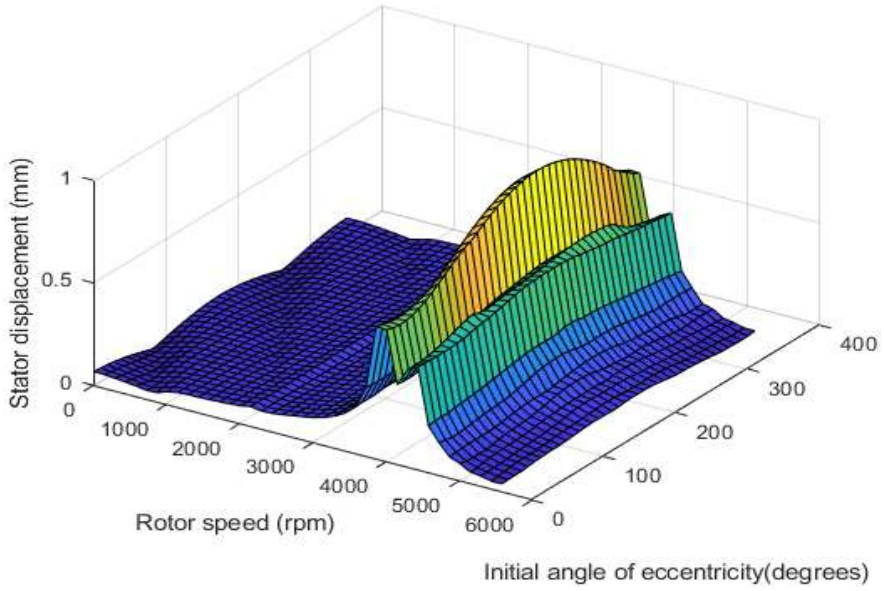

Fig. 9. Dependence of stator vibrations on the angle of eccentricity under the total action of mechanical and magnetic dynamic eccentricity

Conclusion

In this work, a 8 DOF model of the dynamics of an induction motor was created, which takes into account:

- eccentricity of rotor mass; static and dynamic magnetic eccentricity of the rotor;
- influence of the gyroscopic moment of the rotor;
- uneven stiffness of the stator resistance, their number and places of attachment to the stator.

The results of numerous experiments have shown the effectiveness of the model for analyzing the frequency response of the induction motor and its critical speeds, studies of longitudinal oscillations and stator turns, the influence of mass eccentricity and magnetic eccentricity. It is shown that the eccentricity of rotor mass under certain conditions can both increase and decrease the vibrations caused by UMP.

The model can be useful for the study of diagnostic features in vibration diagnostics of electrical machines.

REFERENCES

1. Popa, L.M., Jensen, B.B., Ritchie, E., et al. (2003). Condition monitoring of wind generators. 38th IAS Annual Meeting on Conf. Record of the Industry Applications Conf., Salt Lake City, Utah, USA, vol. 3, pp. 1839– 1846

2. Liu, Y, Chen, Z, Hua, X, Zhai, W. (2022) Effect of rotor eccentricity on the dynamic performance of a traction motor and its support bearings in a locomotive. Proceedings of the

Institution of Mechanical Engineers, Part F: Journal of Rail and Rapid Transit. 236(9):1080-1090.

3. Michon, M., Holehouse, R.C., Atallah, K., et al. (2014). Effect of rotor eccentricity in large synchronous machines. IEEE Trans. Magn. 50(11), pp. 1 – 4

4. Richard N. Bell et al. (1985) Report of large motor reliability survey of industrial and commercial installations. Part II. IEEE Trans. Ind. Appl. 21(4), pp. 865-872

5. Cornell, E. P., Owen, E. L., Appiarius, J. C., McCoy, R. M., Albrecht, P. F., and Houghtaling, D. W. (1982). Improved motors for utility applications. Final report. United States: N. p., Web

6. Bellini, A., Immovilli, F., Rubini, R., Tassoni, C. (2008). Diagnosis of bearing faults of induction machines by vibration or current signals: A critical comparison. In: Industry Applications Society Annual Meeting. IAS'08. IEEE, 2008, pp. 1-8

7. Chuan, H., & Shek, J. K. (2018). Calculation of unbalanced magnetic pull in induction machines through empirical method. IET Electric Power Applications, 12(9), 1233-1239.

8. Salah, A. A., Dorrell, D. G., Guo, Y. (2019). A Review of the Monitoring and Damping Unbalanced Magnetic Pull in Induction Machines Due to Rotor Eccentricity. In IEEE Transactions on Industry Applications. 55(3). pp. 2569-2580.

9. Wang, Z., He, W., Du, S., & Yuan, Z. (2021). Study on the unbalanced fault dynamic characteristics of eccentric motorized spindle considering the effect of magnetic pull. Shock and Vibration. pp. 1-12.